Indian Academy of Sciences Conference Series (2020) 3:1
DOI: 10.29195/iascs.03.01.0011

Spatial feedback control on multistability in hidden attractors

SHIVA DIXIT[1], M. PAUL ASIR[1], AWADESH PRASAD[2],
NIKOLAY V. KUZNETSOV[3,4] and MANISH DEV SHRIMALI[1,*]

[1] Department of Physics, Central University of Rajasthan, Ajmer, India
[2] Department of Physics & Astrophysics, University of Delhi, Delhi, India
[3] Saint-Petersburg State University, St. Petersburg, Russia
[4] Department of Mathematical Information Technology, University of Jyväskylä, Jyväskylä, Finland
*Corresponding author. E-mail: shrimali@curaj.ac.in

Abstract. We propose an intermittent spatial feedback scheme to control the hidden dynamics of the radio-physical oscillator model with coexisting attractors. The feedback is active only in the part of the state-space and inactive in the rest of the regions. We found that this dynamic feedback scheme is effective in controlling the multistability as well as the hidden dynamics of the model. The eminence of the proposed method lies in the fact that the transition to monostable oscillating states and the steady state occurs even for the smaller feedback strength. The elimination of the multiple states and the steady state transitions were affirmed by calculating the basin stability measure and bifurcation diagrams. We show that for suitable feedback active region and the feedback strength the dynamics of the model can be controlled efficiently.

Keywords. Hidden attractors; spatial feedback; multistability.

PACS Nos **05.45.-a; 05.90.+m**

1. Introduction

Multistability refers to the coexistence of multiple asymptotic states in a dissipative system for a given set of parameters [1–4]. It is an exciting phenomenon that possesses wide relevance in physics [5, 6], chemistry [7, 8], biology [9, 10], neuroscience [11, 12], ecosystems [13, 14] and climate dynamics [15, 16]. Multistable systems are extremely sensitive to initial conditions and hence their basin of attraction is complexly interwoven with fractal boundaries [17]. From the perspective of the application, multistability [18] often needs to be controlled to attain the desired dynamical state. Certain strategies have been proposed so far that can be broadly classified into *feedback* and *non-feedback* methods [19]. A feasible way to control multistability without feedback is to apply a small external perturbation to the trajectory until it settles down to the desired state or a basin. This sort of attractor selection using short impulse has been done in both discrete [20, 21] and continuous systems [22, 23]. Another way of eliminating the multiple coexisting states is to add the pseudo-periodic forcing (periodic drive with a small component of chaotic/random drive) [24, 25] or the harmonic perturbations [26, 27] to the system variable. The mechanism of attractor selection with these methods is related to the annihilation of lesser periodic attractors through the crisis. Subsequently, feedback methods entail the addition of the internal state of the system to itself either instantaneously [28, 29] or with a time delay [30, 31].

Recent findings suggest that multistability is entangled with the occurrence of *hidden* attractors [32–34]. An attractor is known as hidden if its basin of attraction does not intersect and is located far away from the neighborhood of any equilibrium [35, 36]. The study of hidden oscillations spurred its way from its seminal observation in Hilbert's 16th problem associated with two dimensional polynomial flows [37]. Later its detection in Chua's model [38–40], Rabinovich system [41–43], aircraft control system [44] and many others receive attention [45]. A heap of investigation has been pursued to study the multistability in hidden attractors that embodies the identification of coexisting hidden attractors in a simplified Lorenz model [46], multiple hidden attractors in a DC/DC converter that operates in the regime of high feedback gain [47], multistability in radio-physical oscillator system [48] and so on. The time delay induced multistability of hidden attractors in a model describing the release of luteinizing hormone and subsequent negative feedback to the hypothalamic nerve has also been reported [49].

Besides, extreme multistability of hidden attractors has been established in a memristive hyperchaotic system [50] and the improved non-autonomous memristive Fitz–Hugh–Nagumo circuit [51].

Gazing at this wide physical relevance, one can readily realize that it is interesting to explore multistability in hidden attractors and their control strategies [52]. The method namely, *linear augmentation* is proposed to stabilize the hidden oscillations to a fixed point as well as proved to effectively control the multistability in such systems [18, 34]. In addition, a linear feedback controller has been employed to control the coexisting chaotic attractor to a fixed point [53], and the delayed feedback control has also been proven successful in eliminating coexisting hidden attractors [54]. However, all these methods employ continuous feedback to the state variable. Recently, the conception of transient uncoupling has been introduced to enhance synchronization in coupled nonlinear systems [55]. Inspired by this, diverse control schemes were proposed based on constrained interaction in both time and spatial domain to tame the dynamics of self-excited attractors [56–61]. Lately, a scheme of time varying feedback control has been adopted to switch the multistable hidden oscillatory states to monostable periodic oscillations followed by the fixed point [62].

Motivated by these control strategies, we wish to introduce a control scheme, namely, *spatial transient feedback* [63], to tame the coexisting states of a radio-physical oscillator system with hidden dynamics [48]. In this scheme, the feedback is active only in the subset of phase space, which is defined by the threshold, and inactive in the rest of the regions. Since continuous feedback cannot be always implemented or occurr in many biological systems [64], in this paper we are proposing the alternative transient feedback approach. The rest of the manuscript is organized as follows: The radio-physical oscillator model with spatial intermittent feedback for controlling multistability is described in section 2. The results proving the efficiency of the control scheme in eliminating coexisting attractors are presented in section 3. The effect of noise on this model with state-space dependent feedback is discussed in section 4. Summary and conclusions drawn from the present study are given in section 5.

2. Model

We consider a three-dimensional autonomous oscillator system recently proposed by Kuznetsov *et al.* [65, 66].

$$\begin{aligned}\dot{x} &= y,\\ \dot{y} &= (\alpha + z + x^2 - \beta x^4)y - \omega^2 x,\\ \dot{z} &= \mu - x^2 - \epsilon h(z)(z - b),\end{aligned} \tag{1}$$

where b is a control parameter and ϵ is the feedback strength. The feedback strength is proportional to the difference between the state variable z and the fixed point created due to feedback. Without feedback, this system describes a radio-physical oscillator system, where ω is the generator's frequency and β is the degree of sub-criticality. The first two equations resemble the generation of hard oscillations whereas the rechargeable power source is given by the last equation. The charging rate of the power source is the parameter μ, and the system is discharged at the rate proportional to $-x^2$. Here, α is the positive feedback strength for the self-oscillator. By introducing the transient spatial feedback term, we primarily modify the charging and discharging pattern of the generator that leads to the control of multistability. The parameters α, μ and β will be kept constant at $\alpha = 0$, $\mu = 0.9$ and $\beta = 0.5$. Here, the state-space dependent feedback $h(z)$ applied to z variable is defined as

$$h(z) = \begin{cases} 1, & \text{if } z \in R' \\ 0, & \text{if } z \notin R' \end{cases} \tag{2}$$

where $R' \subset R^m$ is a subset of the state-space R^m of the system where feedback is on. Here, the subset R' defines in terms of Δ', which can be written in a normalized form as $\Delta = \Delta'/\Delta_a$, where $\Delta_a = (z_{max} - z_{min})$ is the width of an attractor, and z_{max} and z_{min} are the maxima and minima of the z variable of the attractor [55].

3. Results and discussion

To begin with, we analyze the model eq. (1) with $\epsilon = 0$. In the absence of feedback, the system renders coexisting periodic, quasiperiodic and chaotic states as a function of ω. Also, eq. (1) do not have any fixed points in this regime, and therefore, the attractors found in the model are hidden. We examine the bifurcation scenario of the model at $\epsilon = 0$ to demonstrate the multistability as a function of ω. Figure 1a illustrates the coexistence of states for two different initial conditions $[x_0, y_0, z_0] = [2, 0, 0.7]^T$ and $[-1, 0, 0.5]^T$ in the parametric interval $\omega \in [2, 2.5]$. From figure 1, one can see that until $\omega = 2.1$, there prevails coexisting quasiperiodic and chaotic attractors. A little increase in ω alters the complex dynamics into periodic attractors through period halving bifurcations. In the interval of $\omega \simeq [2.1, 2.18]$ the system settles to the coexisting periodic attractors. The two largest Lyapunov exponents ($\lambda_{1,2}$) of the system are plotted as a function of ω in figure 1b using the initial conditions (2, 0, 0.7) and (−1, 0, 0.5), which also indicate the transition to the different attractors like chaotic. Past $\omega = 2.18$, the system enters a bistable region switching between quasiperiodic and

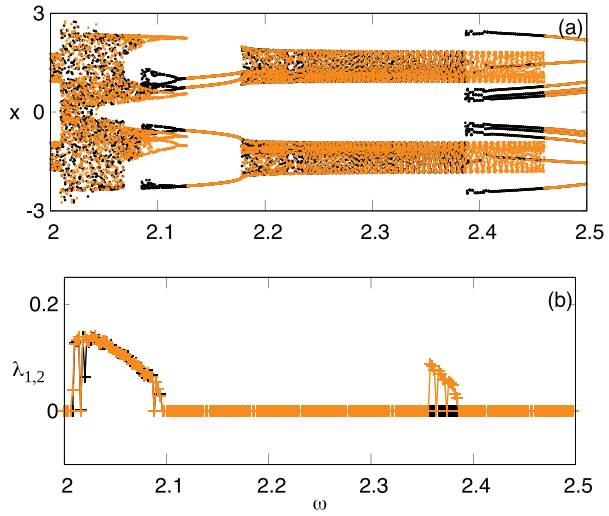

Figure 1. **(a)** Bifurcation diagram depicting the multistability of eq. (1) and **(b)** the two largest Lyapunov exponents of the system with respect to the generator's frequency ω. The parameters are fixed as $\mu = 0.9$, $\beta = 0.5$ and $\epsilon = 0$. The black and orange dots represent two different bifurcation scenarios of the model for the same set of parameters with initial conditions $[x_0, y_0, z_0] = [2, 0, 0.7]^T$ and $[-1, 0, 0.5]^T$ respectively.

chaotic attractors. At $\omega = 2.4$, there is a coexistence of periodic and quasiperiodic dynamics in the model that is evinced by the basin of attraction plot shown in figure 2b1. The basin boundaries between the coexisting attractors entail fractal morphology. The phase portraits of the concurrent quasiperiodic and periodic attractors for the two chosen initial conditions are displayed in figures 2b2 and b3, respectively. In a similar fashion,

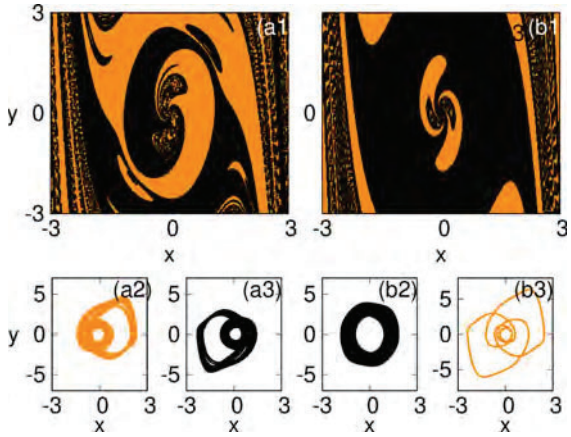

Figure 2. **(a1)** The basin of attraction at $z = 0$ plane at $\epsilon = 0$ for the chaotic attractor (orange) and quasiperiodic attractor (black) at $\omega = 2.077$. The trajectories of **(a2)** chaotic attractor and **(a3)** quasiperiodic attractor. **(b1)** The basin of attraction at $z = 0$ plane at $\epsilon = 0$ for the periodic attractor (black) and quasiperiodic attractor (orange) at $\omega = 2.4$. The trajectories of **(b2)** periodic attractor and **(b3)** quasiperiodic attractor. The other parameters are fixed at $\alpha = 0$, $\mu = 0.9$ and $\beta = 0.5$.

eq. (1) possesses coexisting chaotic and quasiperiodic states at $\omega = 2.077$, and the corresponding basin is shown in figure 2a1. The attractors that prevail in its respective basin can be viewed from figures 2a2 and a3.

To demonstrate the effect of spatially constrained feedback on the control of multistability, we apply conditions given by eq. (2) on the z variable of the model. The feedback is active only at the region R', which is a subset of state-space R^m. R' is defined by the threshold that depends on the values of $z_{\max}$ and $z_{\min}$. When $R' = R$, the scheme imitates a continuous feedback method. We fix the parameters $\mu = 0.9$, $\beta = 0.5$, $b = -1.5$ to study the dynamical transition of the system (eq. (1)) in the $\Delta - \epsilon$ parameter space. Figure 3a shows the different dynamical behaviors exhibited by the system in this parametric space indicated as QP, C, P, SS, which represent quasiperiodic, chaotic, periodic and steady states, respectively. The dynamical regimes are demarcated on the basis of maximal Lyapunov exponents (λ_1). For $\epsilon = 0$ and $\omega = 2.4$, there is a coexistence of quasiperiodic and periodic states in the model. When $\Delta = 1$, the feedback is continuous, which leads to the stabilization of the unstable fixed point created due to feedback after the critical feedback strength $\epsilon_c = 0.5$. In the interval of $0.5 < \Delta < 1$ and $\epsilon > 0.15$, the coexisting attractors of the model are converted into monostable periodic oscillations. Also, one can observe that ϵ_c decreases with an increase in Δ. The one-parameter bifurcation diagram as a function of feedback strength at $\Delta = 0.75$ is given in figure 3b. From the figure, one can evince that after $\epsilon = 0.15$, the quasiperiodic dynamics is controlled to a stable period-1 orbit. Further, at $\Delta = 0.75$, ϵ_c turns out to be 0.6, beyond which the steady state is achieved via Hopf bifurcation. Figures 3d and e depicts the phase portraits of the controlled quasiperiodic and periodic attractors at $\Delta = 0.75$ with $\epsilon = 0.05$ and $\epsilon = 0.4$, respectively. From this, we infer that even the lesser feedback strength $\epsilon \approx 0.05$ is sufficient to eliminate the coexisting periodic attractor from the model. Eventually upon increasing ϵ, the quasiperiodic attractors lose stability and get converted to monostable periodic attractors via period halving bifurcation. With the further increase in ϵ beyond ϵ_c the periodic orbits get stabilized to a fixed point that culminates in the appearance of steady states. These dynamical transitions can be seen from figure 3b.

To evaluate the basin stability of the coexisting attractors as a function of ϵ, we calculated the fraction of initial conditions approaching a specific attractor in the long run. Here the fraction is calculated over the equally distributed initial conditions in the range of $(x_0, y_0) \in [-4, 4] \times [-4, 4]$ with fixed $y_0 = 0.5$ and $\Delta = 0.75$. Figure 3c presents the relative fraction of initial conditions leading to periodic, chaotic, quasiperiodic and steady states. In a narrow window of $\epsilon \in [0.01, 0.1]$

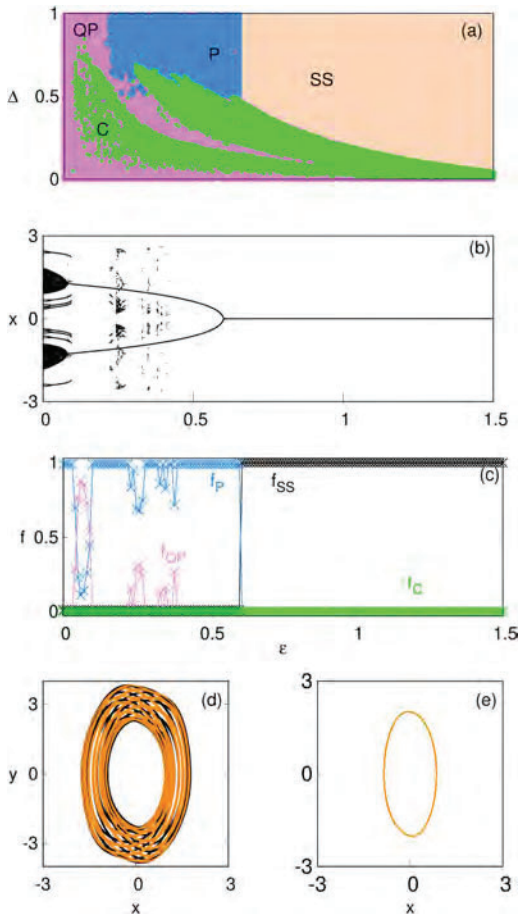

Figure 3. **(a)** The parameter space in (Δ–ϵ) at fixed values of $\mu = 0.9$, $b = -1.5$ and $\omega = 2.4$. The different dynamical regimes are represented as chaotic attractor (C) [green], periodic (P) [blue], quasiperiodic (QP) [purple] and stable steady state (SS) [peach]. The parameter space is calculated using 100 initial conditions distributed randomly on a mesh of $x_0 \in [-2, 2]$, $y_0 \in [-5, 5]$, and $z_0 \in [-2, 2]$. **(b)** Bifurcation diagram as a function of feedback strength at $\Delta = 0.75$. **(c)** Variation of relative basin sizes as a function of feedback strength for chaotic (f_C) [green], periodic along with quasiperiodic (f_P, f_{QP}) [blue, magenta] and steady state attractor (f_{SS}) [black] for 100 initial conditions at $\Delta = 0.75$ and $b = -1.5$, **(d)** controlled quasiperiodic attractors at $\epsilon = 0.05$ and **(e)** periodic attractor $\epsilon = 0.4$. Here, we use two different initial conditions $[x_0, y_0, z_0]^T = [2, 2, 0.5]^T$ and $[-2, -2, 0]^T$.

there is a dominance of quasiperiodic attractor with $f_{QP} \approx 0.91$. When ϵ lies between $0.1 < \epsilon < 0.2$ and $0.4 < \epsilon < 0.6$, we found the completely controlled monostable periodic states with $f_P = 1.0$. Besides, in the interval $0.2 < \epsilon < 0.4$, there is a coexistence of states. Evidently, beyond $\epsilon_c = 0.6$, there is a single globally stable state in the model, which is the steady state which is attested by the rising of f_{SS} to 1.

Similarly, to probe the robustness of the control scheme against the chaotic dynamics, we choose $\omega = 2.077$, where the model exhibits coexisting chaotic attractors. The $\Delta-\epsilon$ parameter space for the chosen ω with the rest of the parameters fixed as in figure 3 is presented in figure 4a. For $\Delta < 0.5$, there is a vivid transition from chaotic to quasiperiodic dynamics accompanied by the coexisting periodic attractors as a function of feedback strength. For $\epsilon > 0.01$ and $\Delta > 0.5$, the coexisting chaotic states are converted into quasiperiodic oscillations. With a further increase in ϵ until $\epsilon_c = 0.5$, monostable periodic oscillations prevail in the system and beyond ϵ_c, the periodic orbits are stabilized

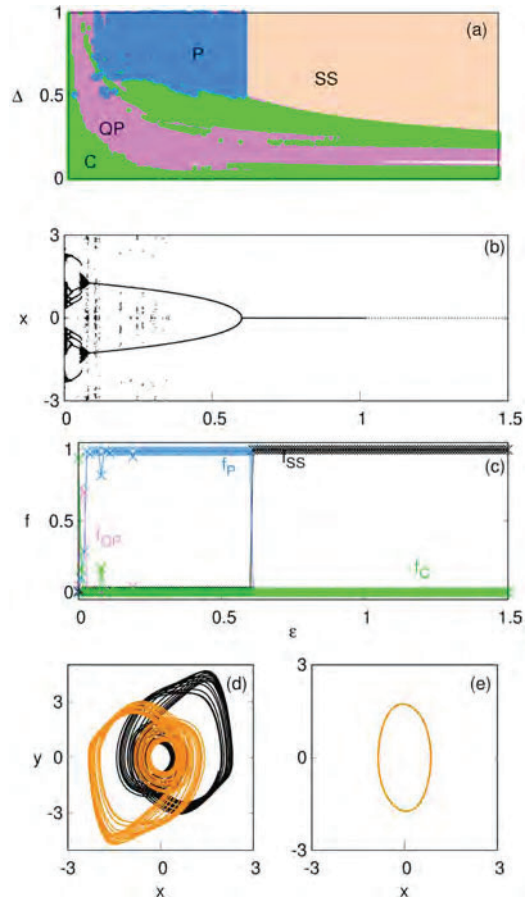

Figure 4. **(a)** The parameter space in (Δ–ϵ) at fixed values of $\mu = 0.9$, $b = -1.5$ and $\omega = 2.077$. The different dynamical regimes are represented as chaotic attractor (C) [green], periodic (P) [blue], quasiperiodic (QP) [purple] and stable steady state (SS) [peach]. The parameter space is calculated using 100 initial conditions distributed randomly on a mesh of $x_0 \in [-2, 2]$, $y_0 \in [-5, 5]$, and $z_0 \in [-2, 2]$. **(b)** Bifurcation diagram as a function of feedback strength at $\Delta = 0.75$, **(c)** variation of relative basin sizes as a function of feedback strength for chaotic (f_C) [green], periodic along with quasiperiodic (f_P, f_{QP}) [blue, magenta] and steady state attractor (f_{SS}) [black] for 100 initial conditions at $\Delta = 0.75$ and $b = -1.5$, **(c)** controlled quasiperiodic attractors at $\epsilon = 0.02$ and **(d)** periodic attractor $\epsilon = 0.4$. Here, we use two different initial conditions $[x_0, y_0, z_0]^T = [2, 2, 0.5]^T$ and $[-2, -2, 0]^T$.

to a fixed point. Likewise, for the case of $\omega = 2.4$, ϵ_c decreases with an increase in Δ. The dynamical transition at $\Delta = 0.75$ with respect to ϵ is elucidated in figure 4b with an aid of a one-parameter bifurcation diagram. The figure depicts that even for small feedback strength $\epsilon > 0.01$, the chaotic dynamics is controlled to the quasiperiodic orbits. A little increase in ϵ leads to a narrow window of chaos that is stabilized to a periodic attractor when ϵ passes 0.1. The clear picture of these transitions can be assimilated by evaluating the basin stability of the different coexisting attractors. The fraction of initial conditions leading to the different asymptotic attractors at $\Delta = 0.75$ is shown in figure 4c. We see that for $\epsilon > 0.03$, the coexisting attractor is converted into a periodic attractor which is confirmed by the elevation of $f_P = 1$. Beyond $\epsilon_c = 0.6$, the system attains a global steady state, depicted as f_{SS} approaches 1. At $\Delta = 0.75$, ϵ_c remains the same for both the cases of ω. Figures 4d and e show the phase portraits of the converted quasiperiodic attractor at $\epsilon = 0.02$ and the controlled period-1 trajectory for $\epsilon = 0.4$ in the x–y plane. Figure 4c emphasizes that a smaller feedback strength is adequate to suppress the chaotic dynamics of the model.

To analyze the influence of the parameter b on the control of multistability and steady state of the model, we plot the b–ϵ space for two values of $\omega = 2.077$ and $\omega = 2.4$ with fixed $\Delta = 0.75$ in figures 5a and b, respectively. The connection between b and the onset of steady state is obtained from the condition of Hopf bifurcation, where the real part of the eigenvalue equals zero at the fixed point $(0, 0, \frac{2\mu}{\epsilon} + b)$. One can see that the monostable periodic dynamics is found at the boundary of the transition to the steady state. In addition, ϵ_c for the transition from periodic to steady state decreases with an increase in b.

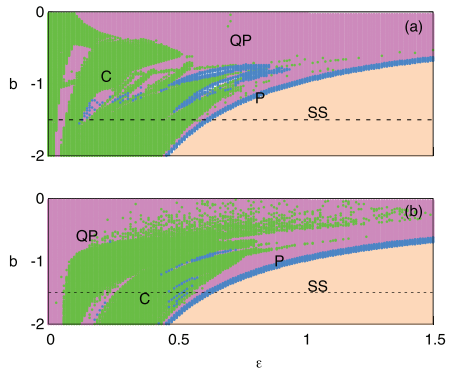

Figure 5. The parameter space in (b, ϵ) for a fixed value of **(a)** $\omega = 2.077$ and **(b)** $\omega = 2.4$. In the green regime, a chaotic attractor (C) exists while the areas with blue and violet colors correspond to the periodic/quasiperiodic (P/QP) and stable steady state (SS), respectively. The other parameters are $\mu = 0.9$ and $\Delta = 0.75$. The dashed line across the figure denotes the chosen $b = -1.5$ for our study.

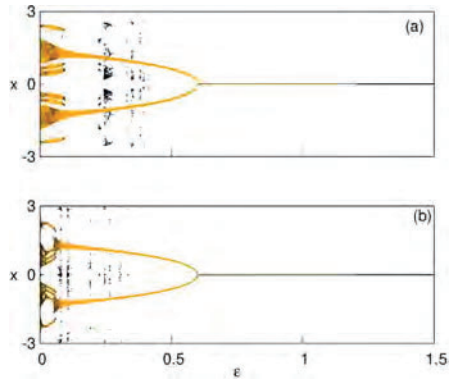

Figure 6. Bifurcation diagram as a function of coupling strength defined by eq. (3) in the presence of noise **(a)** $\omega = 2.4$ and **(b)** $\omega = 2.077$. Black dots denote the bifurcation of the model in the absence of noise. Orange dots represent the bifurcation scenario at $d = 0.015$.

4. Effect of noise

It is reasonable to consider the effect of noise, as the possibility of noise cannot be ruled out for any real system. The dynamics of multistable noisy systems such as a single unit, whole network or formation of clusters has been studied for a long time. The dynamical equations for the system, represented by eq. (3), in the presence of noise can now be written as

$$\begin{aligned} \dot{x} &= y, \\ \dot{y} &= (\alpha + z + x^2 - \beta x^4)y - \omega^2 x, \\ \dot{z} &= \mu - x^2 - \epsilon\, h(z)(z - b) + D\,\eta(t), \end{aligned} \tag{3}$$

where $\eta(t)$ is the Gaussian noise distributed in the interval $[-1, 1]$ and D is its intensity. The other parameters of these equations have the same values as mentioned in section 2. The effect of noise on the system is shown in figure 6 for noise strength ($D = 0.015$ (black dots), 0.5 (orange dots)). The bifurcation diagrams at $\omega = 2.4$ and $\omega = 2.077$ are shown in figures 6a–b. From the figure, one can see that even a feeble noise can eliminate the higher periodic orbits appearing in the narrow window of ϵ. It indicates that noise plays a constructive role in controlling the multistability of the chosen system. Also, the critical ϵ_c for the onset of steady states remains unchanged by the addition of noise.

5. Conclusion

We studied the dynamics of the radio-physical oscillator exhibiting multistable hidden dynamics for the given set of parameters. We found that by imposing the

spatially intermittent feedback one can eliminate the coexisting hidden attractors in this model. The chosen feedback scheme is active only in a certain region of state-space and inactive in the rest of the regions. The control parameter b is found to be inversely proportional to the feedback strength. Furthermore, the significant merit of the adopted control scheme is that it eliminates co-existing attractors in the model as well as ceases the oscillations to a fixed point with lesser feedback strength. By manipulating the control parameters such as the feedback strength (ϵ), region of active feedback (Δ) and the control parameter b we direct the dynamics of the model in the desired way. The adaptability of this method in a pragmatic sense is verified by applying small intensity of noise along with feedback, and we found that the performance of the system does not change on applying a small intensity of noise. Besides, we identify that the inclusion of low intense noise to the model can eliminate the appearence of higher periodic orbits during the transition to a steady state as a function of feedback strength.

Acknowledgements

The authors acknowledge the support from the Department of Science & Technology (DST), India, and the Russian Science Foundation (RSF) for the joint Indo-Russian Collaborative Research project (INT/RUS/RSF/P-18 and 19-41-02002).

References

[1] C Grebogi, E Ott and J A Yorke, *Phys. Rev. Lett.* **56**, 1011 (1986)
[2] C Grebogi, E Ott and J A Yorke, *Nucl. Phys. B* **2**, 281 (1987)
[3] C Grebogi, S W McDonald, E Ott and J A Yorke, *Phys. Lett. A* **99**, 415 (1983)
[4] U Feudel and C Grebogi, *Chaos* **7**, 597 (1997)
[5] T F Arecchi, R Meucci, G Puccioni and J Tredicce, *Phys. Rev. Lett.* **49**, 1217 (1982)
[6] J Kastrup, H T Grahn, K Ploog, F Prengel, A Wacker and E Schöll, *Appl. Phys. Lett.* **65**, 1808 (1994)
[7] M Orban and I Epstein, *J. Phys. Chem.* **86**, 3907 (1982)
[8] I Nagypal and I R Epstein, *J. Phys. Chem.* **90**, 6285 (1986)
[9] M R Guevara, L Glass and A Shrier, *Science* **214**, 1350 (1981)
[10] R P Kline, B M Baker, *Int. J. Bifurcation Chaos* **5**, 75 (1995)
[11] S H Park, S Kim, H B Pyo and S Lee, *Phys. Rev. E* **60**, 2177 (1999)
[12] J Foss and J Milton, *J. Neurophysiol.* **84**, 975 (2000)
[13] N Knowlton, *Am. Zool.* **32**, 674 (1992)
[14] M Scheffer, S Carpenter, J Foley, C Folke and B Walker, *Nature* **413**, 31613 (2001)
[15] A Robinson, R Calov and A Ganopolski, *Nature Climate Change* **2(6)**, 429 (2012)
[16] G Lenderink and R J Haarsma, *J. Phys. Oceanogr.* **24**, 1480 (1994)
[17] M D Shrimali, A Prasad, R Ramaswamy and U Feudel, *Int. J. Bifurcation Chaos* **18**, 1675 (2008)
[18] P R Sharma, M D Shrimali, A Prasad, N V Kuznetsov and G A Leonov, *Eur. Phys. J.: Spec. Top.* **224(8)**, 1485 (2015)
[19] A N Pisarchik and U Feudel, *Phys. Rep.* **540**, 167 (2014)
[20] K Kaneko, *Phys. Rev. Lett.* **63**, 219 (1989)
[21] K Kaneko, *Phys. D* **41**, 137 (1990)
[22] V N Chizhevsky and S I Turovets, *Opt. Commun.* **102**, 175 (1993)
[23] A M Samson, S I Turovets, V N Chizhevsky and V V Churakov, *Sov. Phys.-JETP* **74**, 628 (1992)
[24] L M Pecora and T L Carroll, *Phys. Rev. Lett.* **67**, 945 (1991)
[25] T L Carroll and L M Pecora, *Phys. Rev. E* **48**, 2426 (1993)
[26] A N Pisarchik and B K Goswami, *Phys. Rev. Lett.* **84**, 1423 (2000)
[27] B K Goswami, *Phys. Rev. E* **76**, 016219 (2007)
[28] L Poon and C Grebogi, *Phys. Rev. Lett.* **75**, 4023 (1995)
[29] A Geltrude, K Al Naimee, S Euzzor, R Meucci, F T Arecchi and B K Goswami, *Commun. Nonlinear Sci. Numer. Simul.* **17**, 3031 (2012)
[30] S Rajesh and V M Nandakumaran, *Phys. D* **213**, 113 (2006)
[31] B E Martinez-Zerega, A N Pisarchik and L S Tsimring, *Phys. Lett. A* **318**, 102 (2003)
[32] T Kapitaniak and G A Leonov, *Eur. Phys. J.: Spec. Top.* **224**, 1405 (2015)
[33] N V Kuznetsov and G A Leonov, *IFAC Proceedings Volumes* **47(3)**, 5445 (2014)
[34] P R Sharma, M D Shrimali, A Prasad, N V Kuznetsov and G A Leonov, *Int. J. Bifurcation Chaos* **25(04)**, 1550061 (2015)
[35] D Dudkowski, S Jafari, T Kapitaniak, N V Kuznetsov, G A Leonov and A Prasad, *Phys. Rep.* **637**, 1 (2016)
[36] G A Leonov and N V Kuznetsov, *Int. J. Bifurcation Chaos* **23(01)**, 1330002 (2013)
[37] D Hilbert, *Bull. Am. Math. Soc.* **8(10)**, 437 (1902)
[38] N V Stankevich, N V Kuznetsov, G A Leonov and L O Chua, *Int. J. Bifurcation Chaos* **27(12)**, 1730038 (2017)
[39] G A Leonov, N V Kuznetsov and V I Vagaitsev, *Phys. D* **241(18)**, 1482 (2012)
[40] G A Leonov, N V Kuznetsov and V I Vagaitsev, *Phys. Lett. A* **375(23)**, 2230 (2011)
[41] Z Wei, P Yu, W Zhang and M Yao, *Nonlinear Dyn.* **82(1–2)**, 131 (2015)
[42] M F Danca, N Kuznetsov and G Chen, *Nonlinear Dyn.* **88(1)**, 791 (2017)
[43] N V Kuznetsov, G A Leonov, T N Mokaev, A Prasad and M D Shrimali, *Nonlinear Dyn.* **92(2)**, 267 (2018)

[44] B R Andrievsky, N V Kuznetsov, G A Leonov and A Y Pogromsky, *IFAC Proceedings* **46**(**12**), 75 (2013)
[45] S Jafari, J C Sprott and F Nazarimehr, *Eur. Phys. J.: Spec. Top.* **224**(**8**), 1469 (2015)
[46] C Li and J C Sprott, *Int. J. Bifurcation Chaos* **24**(**03**), 1450034 (2014)
[47] Z T Zhusubaliyev and E Mosekilde, *Math. Comput. Simul.* **109**, 32 (2015)
[48] A P Kuznetsov, S P Kuznetsov, E Mosekilde and N V Stankevich, *J. Phys. A: Math. Theor.* **48**(**12**), 125101 (2015)
[49] Z T Zhusubaliyev, E Mosekilde, A N Churilov and A Medvedev, *Eur. Phys. J.: Spec. Top.* **224**(**8**), 1519 (2015)
[50] B C Bao, H Bao, N Wang, M Chen and Q Xu, *Chaos Solitons Fractals* **94**, 102 (2017)
[51] H Bao, W Liu and M Chen, *Nonlinear Dyn.* **96**(**3**), 1879 (2019)
[52] N K Kamal, V Varshney, M D Shrimali, A Prasad, N V Kuznetsov and G A Leonov, *Nonlinear Dyn.* **91**(**4**), 2429 (2018)
[53] S T Kingni, S Jafari, H Simo and P Woafo, *Eur. Phys. J. Plus* **129**(**5**), 76 (2014)
[54] Z Wang, W Sun, Z Wei and S Zhang, *Nonlinear Dyn.* **82**(**1–2**), 577 (2015)
[55] M Schröder, M Mannattil, D Dutta, S Chakraborty and M Timme, *Phys. Rev. Lett.* **115**(**5**), 054101 (2015)
[56] K Yadav, N K Kamal and M D Shrimali, *Phys. Rev. E* **95**(**4**), 042215 (2017)
[57] K Yadav, A Prasad and M D Shrimali, *Phys. Lett. A* **382**(**32**), 2127 (2018)
[58] Z Sun, N Zhao, X Yang and W Xu, *Nonlinear Dyn.* **92**(**3**), 1185 (2018)
[59] A Prasad, *Pramana – J. Phys.* **81**(**3**), 407 (2013)
[60] S S Chaurasia, A Choudhary, M D Shrimali and S Sinha, *Chaos Solitons Fractals* **118**, 249 (2019)
[61] L Chen, C Qiu and H B Huang, *Phys. Rev. E* **79**(**4**), 045101 (2009)
[62] A Sharma, K Yadav, M D Shrimali, A Prasad and N V Kuznetsov, *Eur. Phys. J.: Spec. Top.* **229**, 1245 (2020)
[63] S Dixit, A Sharma, A Prasad and M D Shrimali, *Int. J. Dyn. Control* **7**(**3**), 1015 (2019)
[64] A Sootla, D Oyarzún, D Angeli and G B Stan, *Automatica* **63**, 254 (2016)
[65] A P Kuznetsov, S P Kuznetsov and N V Stankevich, *Commun. Nonlinear Sci. Numer. Simul.* **15**(**6**), 1676 (2010)
[66] A P Kuznetsov, S P Kuznetsov, E Mosekilde and N V Stankevich, *Eur. Phys. J.: Spec. Top.* **222**(**10**), 2391 (2013)